$K\alpha$ hypersatellites of Zr

S. I. Salem and A. Kumar
Department of Physics and Astronomy, California State University, Long Beach, California 90840
(Received 23 May 1983)

The $K\alpha$ hypersatellites $K\alpha_1^h$ and $K\alpha_2^h$ of zirconium were observed in a conventional x-ray spectrum analysis. The energy separation between the hypersatellites and their corresponding diagram lines were measured, and the intensity ratio $I(K\alpha_1^h)/I(K\alpha_2^h)$ was computed. The experimental values are in good agreement with the results of the most advanced calculations, except for the energy of the $K\alpha_2^h$ where the measured value is some 15 eV higher than the theoretical prediction.

INTRODUCTION

The $K\alpha$ hypersatellites arise as a result of $1s \rightarrow 2p$ transitions in an atom with two holes in the $1s$ state: The $k\alpha_1^h$ results from $1s^{-2} \rightarrow 1s^{-1}2p_{3/2}^{-1}$ and the $K\alpha_2^h$ is the result of a $1s^{-2} \rightarrow 1s^{-1}2p_{1/2}^{1}$ transition.

These weak structures have been detected in the x-ray emission spectra of some thirty elements, mostly low-Z elements,[1-4] with a few observations in the radioactive decay of heavy elements.[5-7]

The study of hypersatellites in elements with $30 \leq Z \leq 60$ is scarce,[8] and for the most part, incomplete.[9] Such a study should include the energy separation of the two $K\alpha$ hypersatellites from their corresponding diagram lines, as well as the intensity ratio $I(K\alpha_1^h)/I(K\alpha_2^h)$.

The two most recent and probably most complete calculations are based on the multiconfiguration Dirac-Fock (MCDF),[10] and the Dirac-Hartree-Slater[11] (DHS) models. When Coulomb and Breit energies are included in the DHS model, the results of the two calculations are in very good agreement for medium- and low-Z elements, but differ significantly for elements with $Z > 60$, where uncertainties in the experimental results are too large to decide between the two theories. For low-Z elements, theoretical and experimental values are in good agreement.[12]

EXPERIMENTAL

The experimental approach is essentially the one traditionally used in the study of x-ray emission spectra. The multiple ionization was produced by a monoenergetic, well-collimated beam of electrons that impinged on a clean smooth surface of a water-cooled block of zirconium. The electrons were accelerated by a 40-keV potential provided by a power supply whose output at this load is essentially ripple free. The emission spectrum was analyzed by a flat quartz crystal ($2d = 2.7490$ Å) mounted in a high-angle goniometer. A time selector circuit activated a stepping motor changing the Bragg angle in increments of $\Delta(2\theta) = 10^{-2}$ deg and simultaneously opened the next channel on a Canberra multichannel analyzer where counts detected by a NaI scintillation detector are stored. At each angular position counts were taken for a 5-min time interval.

The spectrometer was energy calibrated using the $K\alpha_1$ characteristic line of Zr as the energy standard; the energy of the hypersatellites was then determined using the Bragg condition. The system was evacuated by a Vacsorb roughing pump and a fast starting triode Vacion pump, resulting in a clean vacuum of the order of 10^{-6} Torr.

RESULTS

The results of this work are shown in Fig. 1 and in Table I. Figure 1 is one of several spectra of the K hypersatellites of Zr that were recorded and analyzed. Data are initially collected by stepping the spectrometer, thus furnishing intensity as a function of angular positions. By calibrating the spectrometer at the position of the $K\alpha_1$ line of Zr, the angular position of the $K\alpha_1^h$ and $K\alpha_2^h$ were accurately determined. The wavelengths of the hypersatellites were then calculated from the Bragg condition and the known value of quartz crystal lattice spacing. These in turn were converted into energies, $E\lambda = 12\,398.135$ eV Å, resulting in the values shown in Fig. 1, and in Table I.

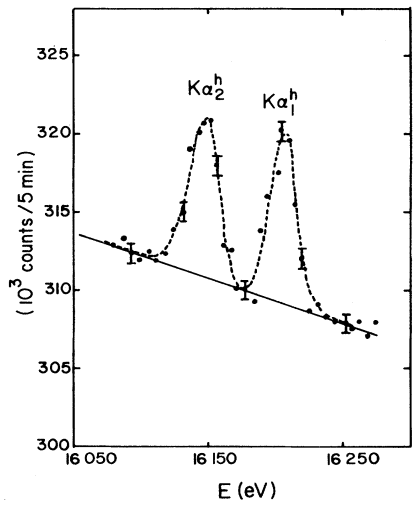

FIG. 1. Hypersatellites, $K\alpha_1^h$ and $K\alpha_2^h$ of Zr plotted as a function of energy.

TABLE I. The energies (in eV) and the relative intensities of the $K\alpha$ hypersatellites of Zr and Mo.

		Energy separation (eV)			$\frac{I(K\alpha_1^h)}{I(K\alpha_2^h)}$		
			Theory[a]			Theory	
Element	Designation	Measured	MCDF	DHS	Measured	MCDF	DHS
Zr	$E(K\alpha_1^h)-E(K\alpha_1)$	434.40±9	437	438.9	1.07±0.2	1.02	1.04
	$E(K\alpha_2^h)-E(K\alpha_2)$	454.50±9	434	439.1			
Mo[b]	$E(K\alpha_1^h)-E(K\alpha_1)$	466.9 ±8	467	465	1.10±0.2	1.13	1.15
	$E(K\alpha_2^h)-E(K\alpha_2)$	473.9 ±8	458	463			

[a]Theoretical values, except for DHS values for Zr were taken from Figs. 2 and 3.
[b]Experimental values for Mo are from Ref. 8.

The reported uncertainties are due to the limit of accuracy with which the position of the $K\alpha_1$ diagram line as well as the positions of the hypersatellites can be determined. The energy separation is simply the difference in the measured energies of the hypersatellites and the known energies of the corresponding diagram lines.[13] The results of this experiment and those reported in Ref. 8 are in excellent agreement with theoretical results in the case of $E(K\alpha_1^h)-E(K\alpha_1)$, Fig. 2, where the two theories differ by 1–2 eV only. The results of Ref. 9 are also in good agreement with theory. In the case of indium, the energy separation was reported with an uncertainty of ±1.3 eV for both $K\alpha_1^h$ and $K\alpha_2^h$, hence the lack of error bars.

In the case of $E(K\alpha_2^h)-E(K\alpha_2)$, the experimental values for both Zr and Mo are some 15 eV higher than theoretical predictions. This is significant because an experiment which provides presumably accurate results in the case of $E(K\alpha_1^h)-E(K\alpha_1)$ is not expected to give such inaccurate values for $E(K\alpha_2^h)-E(K\alpha_2)$. Furthermore it should be noted that the theoretical values of $E(K\alpha_1^h)-E(K\alpha_1)$ are larger than $E(K\alpha_2^h)-E(K\alpha_2)$ for all elements except for those with $40 \leq Z \leq 45$ where the two values are about equal,[11] and the results of DHS are some 3–5 eV higher than those of MCDF in this region of atomic number. More accurate data is needed in this range of atomic number, not only to resolve the difference between the two theories, but to provide an incentive for additional theoretical refinements.

The intensity ratio of the diagram lines $K\alpha_2/K\alpha_1$ has been thoroughly studied over the entire range of atomic numbers, and theories and experiments are in excellent agreement.[14,15] But in the production of hypersatellites, the $1s$ state is initially devoid of electrons, and the physical conditions that govern transition rates are different from those governing the emission of diagram lines. For low-Z elements, if one assumes pure LS coupling, there would be only one allowed electric dipole transition, $1S \rightarrow 1P$, which gives rise to $K\alpha_2^h$. The fact that $K\alpha_1^h$ is not zero indicates that some mixing takes place.

On the other hand, for high-Z elements, where the $2p$

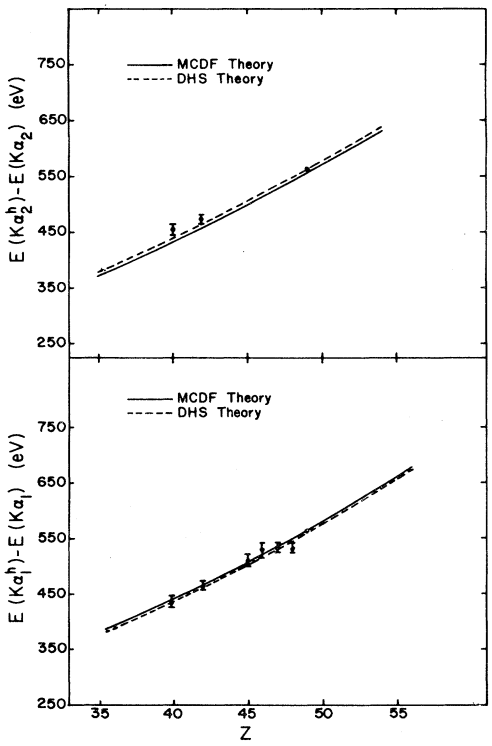

FIG. 2. Energy separation $E(K\alpha_2^h)-E(K\alpha_1^h)$ above, and $E(K\alpha_1^h)-E(K\alpha_1)$ below are plotted as functions of atomic numbers. Values for Zr are from this work, Mo from Ref. 8 and the rest from Ref. 9. Solid curve from Ref. 10 and dashed curve from Ref. 11.

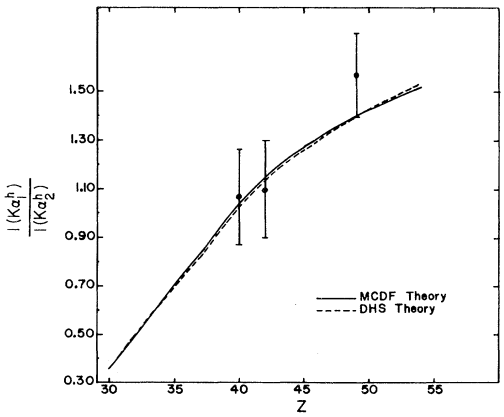

FIG. 3. Relative intensity of the $K\alpha$ hypersatellites plotted as a function of atomic numbers. The value of Zr is from this work, Mo from Ref. 8, and In from Ref. 9. Solid curve from Ref. 10 and dashed curve from Ref. 11.

spin-orbit interaction is strong, one approaches the *jj*-coupling limit[16] where the ratio $I(K\alpha_1^h)/I(K\alpha_2^h) \rightarrow 2$ is in agreement with the results of MCDF computations, and at variance with the results of DHS which predicts a value of about 1.6 for this ratio in that region.

For elements with medium atomic number, the results of the two theories and the available experimental values are shown in Fig. 3. All three experimental points are reported with some 20% uncertainty. Large uncertainties are intrinsic in the intensity measurements of weak lines superimposed on intense background.

ACKNOWLEDGMENTS

We wish to acknowledge the support of the California State University, Long Beach Foundation and the assistance of Mr. B. A. Scott and Mr. W. J. Maxey in building some of the electronic components.

[1]D. J. Nagel, A. R. Knudson, and P. G. Burkhalter, J. Phys. B 8, 2779 (1975).
[2]O. Keski-Rahkonen, J. Saijonmaa, M. Suvanen, and A. Servomaa, Phys. Scr. 16, 105 (1977).
[3]J. Ahopelto, E. Rantavuori, and O. Keski-Rahkonen, Phys. Scr. 20, 71 (1979).
[4]J. P. Briand, A. Touati, M. Frilley, P. Chevalier, A. Johnson, J. P. Rozet, M. Tavernier, S. Shafroth, and M. O. Krause, J. Phys. B. 9, 1055 (1976).
[5]J. P. Desclaux, Ch. Briancon, J. P. Thibaud, and R. J. Walen, Phys. Rev. Lett. 32, 447 (1974).
[6]K Schreckenbach, H. G. Börner, and J P. Desclaux, Phys. Lett. 63A, 330 (1977).
[7]J. P. Briand, P. Chevalier, A. Johnson, J. P. Rozet, M. Tavernier, and A. Touati, Phys. Lett. 49A, 51 (1974).
[8]S. I. Salem, Phys. Rev. A 21, 858 (1980).
[9]C. W. E. Van Eijk, J. Wijnhorst, and M. A. Popelier, Phys. Rev. C 19, 1017 (1979); C. W. E. Van Eijk *et al.*, Phys. Rev. A 24, 854 (1981).
[10]T. Åberg and M. Suvanen, *Advances in X-Ray Spectroscopy*, edited by C. Bonnelle and C. Mande (Pergamon, New York, 1980).
[11]M. H. Chen, B. Crasemann, and H. Mark, Phys. Rev. A 25, 391 (1982).
[12]S. I. Salem, A. Kumar, B. L. Scott, and R. D. Ayers, Phys. Rev. Lett. 49, 1240 (1982).
[13]J. A. Bearden Rev. Mod. Phys. 39, 78 (1967).
[14]S. I. Salem, S. L. Panossian, and R. A. Krause, At. Data Nucl. Data Tables 14, 91 (1974).
[15]J. H. Scofield, At. Data Nucl. Data Tables 14, 121 (1974).
[16]T. Åberg, J. P. Briand, P. Chevalier, A. Chetioui, J. P. Rozet, M. Tavernier, and A. Touati, J. Phys. B 9, 2815 (1976).